BRIEF COMMUNICATIONS

The purpose of this Brief Communications section is to present important research results of more limited scope than regular articles appearing in Physics of Fluids. Submission of material of a peripheral or cursory nature is strongly discouraged. Brief Communications cannot exceed four printed pages in length, including space allowed for title, figures, tables, references, and an abstract limited to about 100 words.

The threshold of the instability in miscible displacements in a Hele–Shaw cell at high rates

E. Lajeunesse, J. Martin, N. Rakotomalala, and D. Salin
Laboratoire Fluides Automatique et Systèmes Thermiques, Universités P. et M. Curie and Paris Sud, C.N.R.S. (UMR 7608), Bâtiment 502, Campus Universitaire, 91405 Orsay Cedex, France

Y. C. Yortsos
Department of Chemical Engineering, University of Southern California, Los Angeles, California 90089-1211

(Received 27 January 2000; accepted 7 November 2000)

For sufficiently large viscosity ratios and injection rates, miscible displacements in a vertical Hele–Shaw cell at high rates become unstable, leading to three-dimensional (3D) fingering patterns. Below the instability threshold, the base state is 2D in the form of a ''tongue'' of constant thickness. We apply the long wave Saffman–Taylor stability analysis to find an expression for the threshold of instability as a function of the viscosity ratio and the injection rate. The results are in agreement with the experimental data. © *2001 American Institute of Physics.* [DOI: 10.1063/1.1347959]

Introduction. Miscible displacements in a Hele–Shaw cell and/or a tube have recently been extensively investigated numerically,[1,2] theoretically[3,4] and experimentally.[4–6] At sufficiently high flow rates, diffusion is negligible and a well-defined interface exists between the two fluids, the shape of which is governed only by viscous and buoyant forces. In the experiments reported in Ref. 6 a vertical Hele–Shaw cell is filled with an initial fluid 1. The cell consists of two parallel plates of length $L=80$ cm (direction x) and width $W=10$ cm (direction y), separated by a spacer, ensuring a gap of uniform thickness $b=1.00$ mm or 1.92 mm (direction z). A lighter and less viscous fluid 2, miscible to the fluid in place, is injected at the top of the cell at a constant flow rate, generating a downward displacement. This displacement is buoyant-stable but viscous-unstable. The two control parameters are the viscosity ratio and the buoyancy-normalized flow rate defined, respectively, by

$$M=\frac{\eta_1}{\eta_2} \quad \text{and} \quad U=\frac{\eta_1 q}{k\Delta\rho g}=\frac{q}{V_g}, \tag{1}$$

where η denotes viscosity, q the gap-averaged flow velocity, $k=b^2/12$, the permeability of the cell, $\Delta\rho=\rho_1-\rho_2>0$, the density difference between initial and injected fluids and $V_g\equiv k\Delta\rho g/\eta_1$, the buoyancy-driven velocity. At low flow rates (but still high enough for $\mathrm{Pe}=qb/D\gg 1$, where D is the molecular diffusivity), the interface between the fluids spans symmetrically across the gap, and has a 2D tonguelike shape in the $x-z$ plane, which is invariant in the transverse $-y$ direction. However, when the viscosity ratio is larger than a critical value, $M>M_C$, and at the same time the normalized velocity exceeds an M-dependent threshold, $U_C(M)$, the tongue becomes unstable leading to a 3D fingering pattern.[6] The purpose of this note is to derive theoretical expressions for the viscosity and velocity thresholds.

The base state. Below the onset of instability, the 2D base state was found experimentally[4] to consist of a (shocklike) tongue of the displacing fluid of a constant relative thickness, t, propagating at a constant velocity, V_S, leaving behind a film of the initial fluid of relative thickness $1-t$ (Fig. 1). Except near the leading edge at the tip of the tongue, this base state is a 2D parallel flow, in which the pressure is constant across the gap and along the transverse $-y$ direction, but varies along the vertical, $-x$, direction. Far from the tip, the velocity field consists of Poiseuille flow parabolic segments.[3,4] Hence, the gap-averaged velocity, f_i, for each fluid i $(i=1,2)$ can be derived,

$$f_i=-\frac{k}{\tilde{\eta}_i}(\partial_x P-\tilde{\rho}_i g), \tag{2}$$

where

$$\tilde{\eta}_1(t)=2\eta_1/(t+2)(t-1)^2,$$
$$\tilde{\eta}_2(t)=2\eta_1/t(3+(2M-3)t^2), \tag{3}$$

and

$$\tilde{\rho}_1(t)=\rho_1-3t\Delta\rho/(t+2),$$
$$\tilde{\rho}_2(t)=\rho_1-2t\Delta\rho(3+(M-3)t)/(3+(2M-3)t^2). \tag{4}$$

The base state was found to exist within a certain region of M and U values. This region is delineated in Fig. 2 by a lower and an upper boundary. The dashed line is the lower boundary of the region. It is defined by the condition that the shape of the interface between the two fluids changes from

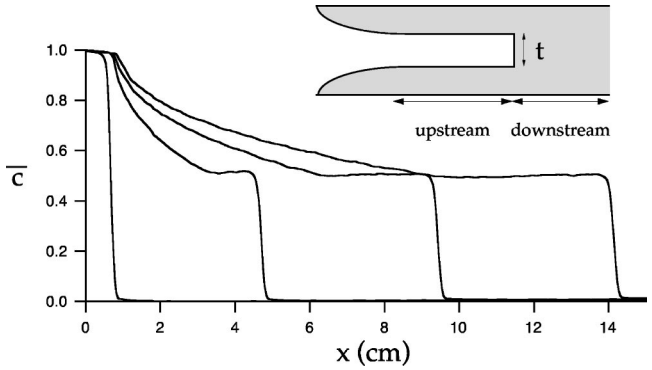

FIG. 1. Gap-averaged concentration profiles at four different time intervals ($\Delta t = 20$ s) for $M = 23.6$ and $U = 1.2$, near the onset of 3D instability (note that for this particular viscosity ratio, $U_{23} = 0.6$ and $U_C = 1.3$). The base state is a frontal shock of relative thickness t and of velocity V_S, as shown schematically in the upper right corner.

one involving two self-spreading segments and an interior shock (and which characterizes the regime below this boundary), to a frontal shock followed upstream by a self-spreading segment (and which is the base state under consideration, Fig. 1). The region has an upper boundary defined in Fig. 2 by the experimental data, which corresponds to the onset of the 3D instability. The lower boundary, denoted as U_{23}, was analytically determined in Ref. 4. The objective of this note is to derive an analytical expression for the upper boundary, which is currently unknown. For this, we will make use of the findings from our previous work.[4]

Between the two boundaries, the thickness of the tongue, t, was found experimentally to remain approximately constant, as a function of U, and to vary only as a function of M. Although we have no analytical theory at present to explain this finding, we will combine it with the fact that a full analytical description is available for the flow below this region, and hence at the limiting boundary U_{23}.[4] Thus, we obtain for t at U_{23}, and by extension for t in the entire region of the base state, the expression

$$t(M) = \frac{2M-3}{4M-3}; \quad M \geqslant \frac{3}{2}. \tag{5}$$

Figure 3 shows a comparison between Eq. (5) and the experimental data. The agreement between the two is quite good. Equation (5) shows that the shocklike base state is possible only if $M \geqslant 3/2$, and that t vanishes as M approaches 3/2.

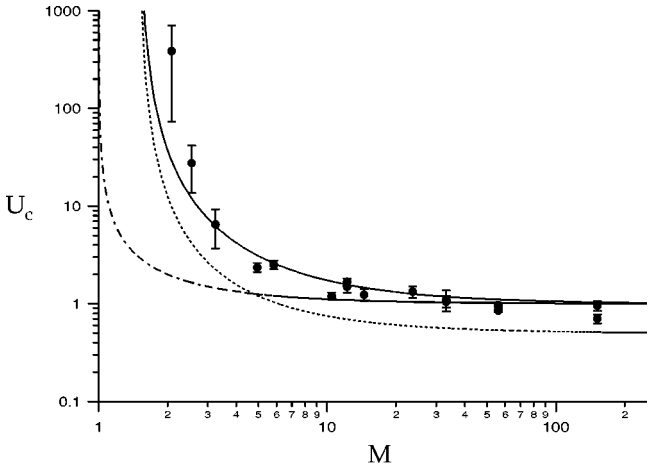

FIG. 2. Comparison between the experimental results for the instability threshold (circles) and its theoretical estimate, Eq. (15) (full line). The small dashed line corresponds to $U_{23}(M)$ obtained from Ref. 4. The dash-dot line corresponds to the threshold calculated by setting $t = 1$ in Eq. (14).

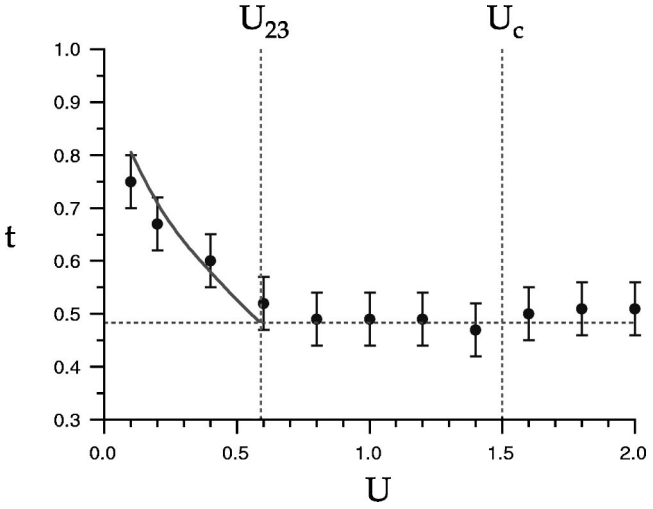

FIG. 3. Comparison between the thickness t of the base state (frontal shock) before the onset of instability (circles) and the calculated values from Eq. (5) (solid line).

The base state is analogous to the one studied in the Appendix of the classical paper by Saffman and Taylor (ST).[7] In the following, we will apply their long wave analysis to determine its stability.

Instability thresholds. Consider, first, the stability of the more general base state illustrated in Fig. 4, where the upstream and downstream far field regions, denoted below by the subscript j ($j = u, d$), consist of a central layer of displacing fluid 2, with relative thicknesses t_u and t_d, respectively. The two regions are separated by a sharp front, moving with the velocity

$$V_S = \frac{f_2(t_d) - f_2(t_u)}{t_d - t_u} = \frac{f_1(t_d) - f_1(t_u)}{(1-t_d) - (1-t_u)}. \tag{6}$$

A combination of Eqs. (2)–(4), (6) leads to the following pressure gradients at the interface:

$$(\partial_x P)_j = \rho_j g - \eta_j V_S / k, \quad j = u, d, \tag{7}$$

where the quantities ρ_j and η_j depend on both t_u and t_d. In each far region, the gap-averaged velocity q, obtained from $q = f_1 + f_2$, obeys a Darcy-type equation

$$q = -\frac{k}{\eta_{\text{eff}}}(\partial_x P - \rho_{\text{eff}} g), \tag{8}$$

where η_{eff} and ρ_{eff} depend on the local value of t [see Eqs. (2)–(4)]. This equation, combined with the parallel flow hypothesis (uniform t) and mass conservation, leads to the Laplacian $\nabla^2 P = 0$. Thus, the problem becomes identical to the

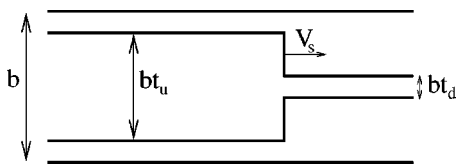

FIG. 4. Sketch of the base state assuming parallel flow: The displacing fluid occupies a central layer of relative thickness t_u and t_d, upstream and downstream of the front, respectively. The front moves at velocity V_S.

ST problem. Consider, next, the rate of growth of a sinusoidal perturbation of the front, $x=a\exp(iny+\sigma t)$. By applying the conditions that the pressure perturbation vanishes at infinity, the pressure gradient obeys Eq. (7) at the interface, with $V_S=V_{So}+a\sigma\exp(iny+\sigma t)$, and that the pressure is continuous on both sides of the front, we obtain the following dispersion relation between the growth rate σ and the wave vector n

$$\frac{\sigma}{n}(\eta_d+\eta_u)=(\eta_d-\eta_u)(V_S-V_C), \tag{9}$$

where $V_C=[k(\rho_d-\rho_u)g/\eta_d-\eta_u]$ is the critical front velocity.[8] Alternatively, the dispersion relation may be expressed in terms of the pressure gradients in the far regions, namely

$$\frac{\sigma}{n}(\eta_d+\eta_u)=k[(\partial_x P)_u-(\partial_x P)_d]. \tag{10}$$

Physically, instability occurs when the absolute value of the pressure gradient downstream is larger than its value upstream. By eliminating the pressure gradients using Eq. (8), and introducing the normalized flow rate $U=q/V_g$, one obtains

$$\frac{\sigma}{n}=\alpha(U-U_C), \tag{11}$$

where

$$U_C=\frac{\eta_1[\rho_{\text{eff}}(t_d)-\rho_{\text{eff}}(t_u)]}{[\eta_{\text{eff}}(t_d)-\eta_{\text{eff}}(t_u)]\Delta\rho} \quad \text{and}$$
$$\alpha=V_g\frac{\eta_{\text{eff}}(t_d)-\eta_{\text{eff}}(t_u)}{\eta_d+\eta_u}. \tag{12}$$

In terms of t_u and t_d, the expression of U_C is $U_C(t_u,t_d)$

$$=\frac{(2M-3)(t_u^2+t_d^2+t_dt_u)+3-3(M-1)t_ut_d(t_u+t_d)}{2(M-1)(t_u^2+t_d^2+t_dt_u)}. \tag{13}$$

Thus, for our particular base state ($t_d=0$, $t_u=t$) the dispersion relation finally reads

$$\frac{\sigma}{n}=V_g(U-U_C)\frac{(M-1)[3+(2M-3)t^2]t^3}{2[1+(M-1)t^3][2+(M-1)t^3]}$$
$$\text{where}\quad U_C=\frac{(2M-3)t^2+3}{2(M-1)t^2}. \tag{14}$$

Given the requirement Eq. (5) for the existence of the base state, $M\geqslant 3/2$, Eq. (14) shows that instability occurs when $(U-U_C)t>0$, namely, it requires the simultaneous conditions $M\geqslant 3/2$ and $U>U_C$. Combining Eq. (5) with Eq. (14), we then obtain the final expression for the boundary delineating the onset of instability

$$U_C(M)=\frac{M(M^2+\frac{3}{2}(M-\frac{3}{2}))}{(M-1)(M-\frac{3}{2})}. \tag{15}$$

Equation (15) is an analytical expression for the upper boundary of the region discussed in Fig. 2. The resulting curve is plotted in the M, U plane of Fig. 2 as a solid line. Comparison with the experimental data shows good agreement between theory and experiment. In particular, this expression gives rise to a threshold viscosity ratio of $M_C=3/2$, below which no viscous fingering was observed experimentally[6] (for this high rate miscible displacement). We remark that our theoretical expression, derived in the long wave limit, gives *a priori* an upper bound to the experimental critical velocity, as the flow could be destabilized for smaller velocities, at smaller wavelengths. In addition, the selected wave length in the fully-developed instability at later stages, $\lambda\sim 5\ b$,[6] does not clearly satisfy the long wavelength constraint, $\lambda\gg b$. However, this selection occurs in the late, nonlinear regime, which is not necessary relevant to the early-stage linear destabilization analyzed here. The analytical expressions do provide a good prediction for the velocity threshold, U_C, and a satisfactory account of the variation of the tongue thickness with M and its vanishing at $M_C=3/2$. By contrast, if we were to neglect the $t(M)$ dependence, and use constant t in Eq. (14), the results are less satisfactory. Plotted in Fig. 2 as a dash-dot line is the resulting expression for the specific case $t=1$, and where, now, $U_C=M/(M-1)$. It is clear that, although fitting the data well at large M, this curve fails to provide an adequate match at smaller values of M.

Conclusions. In this note, we studied the onset of instability for a vertical miscible displacement in a Hele–Shaw cell at high rates. Using a base state which is viscosity ratio-dependent, and determined analytically, we applied the long wave Saffman–Taylor stability analysis to obtain explicit expressions for the instability thresholds M_C and $U_C(M)$. The results are in good agreement with the experiments. In particular, they also predict that in the absence of buoyancy a value of M larger than 3/2 is required for instability to occur.

ACKNOWLEDGMENTS

One of the authors (Y.C.Y.) would like to acknowledge support from Grant No. DE-AC26-99BC15211 of the Department of Energy. The contribution of NATO Grant No. GRC973049 is also acknowledged.

[1] C. Y. Chen and E. Meiburg, ''Miscible displacements in capillary tubes. Part 2. Numerical simulations,'' J. Fluid Mech. **326**, 57 (1996).
[2] N. Rakotomalala, D. Salin, and P. Watzky, ''Miscible displacement between two parallel plates: BGK lattice gas simulations,'' J. Fluid Mech. **338**, 277 (1997).
[3] Z. Yang and Y. C. Yortsos, ''Asymptotic solutions of miscible displacements in geometries of large aspect ration,'' Phys. Fluids **9**, 286 (1997).
[4] E. Lajeunesse, J. Martin, N. Rakotomalala, D. Salin, and Y. C. Yortsos, ''Miscible displacements in a Hele–Shaw cell at high rates,'' J. Fluid Mech. **398**, 299 (1999).
[5] P. Petitjeans and T. Maxworthy, ''Miscible displacements in capillary tubes. Part 1. Experiments,'' J. Fluid Mech. **326**, 37 (1996).
[6] E. Lajeunesse, J. Martin, N. Rakotomalala, and D. Salin, ''3D instability of miscible displacements in a Hele–Shaw cell,'' Phys. Rev. Lett. **79**, 5254 (1997).
[7] P. G. Saffman and G. I. Taylor, ''The penetration of a fluid into a porous medium or Hele–Shaw cell containing a more viscous liquid,'' Proc. R. Soc. London, Ser. A **245**, 312 (1958).
[8] The dispersion equation derived in the Appendix of Ref. 7 can be recovered by Eq. (9) with $t_u=t$ and $t_d=0$, provided the following misprints in Ref. 7 are corrected: In Eq. (A3), ρ_1 in the denominator should be replaced by ρ_2, in the expression for A in Eq. (A6), $\mu_1 t$ should be replaced by $\mu_1 t^2$, while the viscosity of the ''effective invading fluid'' should be taken equal to $\mu_2'=2\mu_1/(3+(2M-3)t^2)$ instead of μ_2.